Mode stability analysis in the beam–wave interaction process for a three-gap Hughes-type coupled cavity chain*

Luo Ji-Run(罗积润)[a)†], Cui Jian(崔 健)[b)], Zhu Min(朱 敏)[a)], and Guo Wei(郭 炜)[a)]

[a)] *Institute of Electronics, Chinese Academy of Sciences, Beijing* 100190, *China*

[b)] *College of Electronic Information and Control Engineering, North China University of Technology, Beijing* 100124, *China*

(Received 29 October 2012; revised manuscript received 24 November 2012)

Based on space-charge wave theory, the formulae of the beam–wave coupling coefficient and the beam-loaded conductance are given for the beam–wave interaction in an N-gap Hughes-type coupled cavity chain. The ratio of the non-beam-loaded quality factor of the coupled cavity chain to the beam quality factor is used to determine the stability of the beam–wave interaction. As an example, the stabilities of the beam–wave interaction in a three-gap Hughes-type coupled cavity chain are discussed with the formulae and the CST code for the operations of the 2π, π, and $\pi/2$ modes, respectively. The results show that stable operation of the 2π, π, and $\pi/2$ modes may all be realized in an extended-interaction klystron with the three-gap Hughes-type coupled cavity chain.

Keywords: three-gap Hughes-type coupled cavity chain, coupling coefficient, beam-loaded conductance, beam quality factor, stability

PACS: 78.70.Gq, 84.40.–x, 84.40.Fe **DOI:** 10.1088/1674-1056/22/6/067803

1. Introduction

A klystron is a vacuum microwave electron device with high power and high efficiency. However, with an increase in frequency, its geometrical size will decrease, which greatly restricts the power capability and withstand voltage of the device. Extended-interaction klystrons (EIK), based on an extended interaction structure, can achieve high power, wide bandwidth, and high gain in the millimeter/sub-millimeter wavelength range.[1–8] The extended interaction structure is composed of several coupled cavities that strongly couple to each other by slots on the common walls between the adjoining cavities. The enlarged inner surface area of the multi-gap coupled cavity chain can improve the power capacity, and the higher coupling impedance can also compensate for the lower beam conductance, keeping a high efficiency in millimeter-scale circuits. Because of these characteristics, the EIK can have very broad applications, especially in the areas of airborne radars, communications, and electronic countermeasures.

Chodorow and Wessel-Berg[2] analyzed the behavior of the multi-gap coupled cavity chain with extended interaction fields according to space-charge theory, and found that the experimental performances accord well with the theoretical ones. However, their results were obtained based on a one-dimensional grid gap, and the effects of the space-charge parameter on the beam–wave synchronization and coupling in the multi-gap coupled cavity chain were neglected. Because of the coupling between the adjacent cavities, the number of modes in the multi-gap Hughes-type coupled cavity chain will increase with increasing gap number, so stability becomes a key technique issue for the development of the EIK. Preist and Leidigh[9] discussed the beam–wave interaction stability of a three-gap output cavity with the ratio of the loaded quality factor $Q_{\rm L}$ to its value at the resonant point by combining their design and experimental research. Lien and Robinson[10] analyzed the stability in a double-gap coupled cavity output circuit with two-mode overlapping with the beam-loaded conductance based on an equivalent circuit. Quan *et al.*[11] expressed the beam-loaded conductance with an ungridded gap in a double-gap coupled cavity, and used it to determine the stability of the electromagnetic mode. Whereas the gap number was limited to two, and it is difficult to explain the mechanisms of the beam–wave synchronization, coupling and stability in the coupled cavity chain with more gaps.

In this paper, starting from the small signal theory of mono-energetic electron movement, based on the formulae of the beam–wave coupling coefficient and the beam-loaded conductance in an N-gap Hughes-type coupled cavity chain with an electron beam and some electrical parameters obtained using the CST code, the stability of the beam–wave interaction in a three-gap Hughes-type coupled cavity chain will be discussed with the ratio of the non-beam-loaded quality factor of the coupled cavity chain to the beam quality factor in order to better describe the effect of the gap electric field and the coupled cavity chain loss.

2. Model and formulae

Figure 1 shows the model of an N-gap Hughes-type coupled cavity chain. It consists of several Hughes-type coupled

*Project supported by the National Natural Science Foundation of China (Grant No. 11205162).

†Corresponding author. E-mail: luojirun@mail.ie.ac.cn

© 2013 Chinese Physical Society and IOP Publishing Ltd

cavities that strongly couple to each other by a single slot on the common walls between the adjoining cavities in the longitudinal direction, and the adjoining coupling slots are alternately placed with 180° phase difference. Usually, it is considered as a slow-wave structure with the short circuit at two terminals. The standing wave electric field in it is a superposition of the forward wave and the reflected wave with the same amplitude and opposite propagation direction. In Fig. 1, r is the radius of the cavity; r_a and r_c are, respectively, the inner and outer radius of the drift tube; r_s is the radius of the coupling slot center line; d, d_s, and t are, respectively, the gap spacing, the coupling slot width, and the thickness of the cavity wall; θ is the sector angle of the coupling slot; and l_{1j} is the distance between the first gap center and the j-th gap center ($j = 2, 3, 4, \ldots, n$).

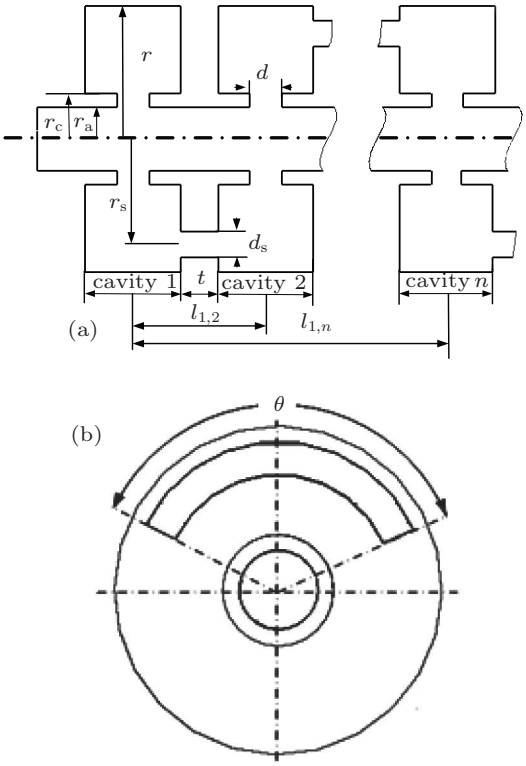


Fig. 1. Model of an N-gap Hughes-type coupled cavity chain: (a) longitudinal section, and (b) crossed section with sector slot.

Based on space-charge wave theory,[2] starting from Maxwell's equations, the equation of electron motion, and the continuity equation, by calculating the complex power extracted from the beam on the gaps, the active power absorbed by the beam P_r and the beam conductance $G_b = 2P_r/V^2$ can be written, respectively, as

$$P_r = \frac{P+P^*}{2} = \frac{V^2}{8Z_0}\left(\left|M(\beta_e-\beta_q)\right|^2 - \left|M(\beta_e+\beta_q)\right|^2\right), \quad (1)$$

$$G_b = \frac{2P_r}{V^2} = \frac{1}{4Z_0}\left(\left|M(\beta_e-\beta_q)\right|^2 - \left|M(\beta_e+\beta_q)\right|^2\right), \quad (2)$$

where $M(\beta_e-\beta_q)$ and $M(\beta_e+\beta_q)$ are, respectively, the coupling coefficient for the fast and slow space-charge wave, which can be expressed as[12–14]

$$M(\beta) = \frac{\sqrt{\dfrac{I_0^2(\gamma(\beta)r_b) - I_1^2(\gamma(\beta)r_b)}{I_0^2(\gamma(\beta)r_a)}}\int_{-\infty}^{+\infty} E(z,r_a)\,e^{æ\beta z}dz}{V}, \quad (3)$$

where $\beta_e = \omega/v_0$, $\beta_q = \omega_q/v_0$, $\gamma(\beta) = \sqrt{\beta^2 - k^2}$, $k = \omega/c$, with v_0 being the velocity of the beam, ω the angle frequency, ω_q the reduced plasma frequency, $I_0(x)$ and $I_1(x)$ are, respectively, the zero-order and first-order modified Bessel function, r_b is the electron beam radius, $Z_0 = (2V_0/I_0)(\beta_q/\beta_e)$ the beam characteristic impedance, $V = \sum_{n=1}^{N}|V_n|$ the effective voltage,[15] V_n the voltage on the n-th gap, and $E(z,r_a)$ the standing wave electric field on the gap at $r = r_a$. For an N-gap Hughes-type coupled cavity chain, $E(z,r_a)$ can be given as

$$E(z,r_a) = \sum_{n=1}^{N} E_n(z - l_{1,n}, r_a). \quad (4)$$

$E_n(z-l_{1,n},r_a)$ is the RF electric field on the n-th gap, so the coupling coefficient on the n-th gap can be defined as

$$M_{g,n} = \frac{\sqrt{\dfrac{I_0^2(\gamma(\beta)r_b) - I_1^2(\gamma(\beta)r_b)}{I_0^2(\gamma(\beta)r_a)}}}{|V_n|} \times \int_{l_{1,n}-d_n/2}^{l_{1,n}+d_n/2} E_n(z-l_{1,n},r_a)\,e^{æ\beta(z-l_{1,n})}dz. \quad (5)$$

The coupling coefficient of the N-gap Hughes-type coupled cavity chain $M_N(\beta)$ can be written as

$$M_N(\beta) = \frac{\sum_{n=1}^{N} M_{g,n}(\beta)V_n\,e^{æ\beta l_{1,n}}}{\sum_{n=1}^{N}|V_n|}. \quad (6)$$

3. Stability of the modes in a three-gap coupled cavity chain

3.1. Definition of stability

In an N-gap coupled cavity chain, there are N cavity modes and $N-1$ slot modes,[16] so it is very important to keep the stability of the operating mode and avoid the oscillation of parasitic modes. Usually, the beam-loaded conductance is used to characterize the stability, which can only reflect the energy exchange between the beam and the gap electric field.[17] The reciprocal of the beam quality factor, Q_b, can show the energy coupling between the beam and the gap electric field (G_b) and the effect of the gap electric field on the stability (R/Q, characteristic impedance) at the same time. However, the instability of the mode is still related to the quality factor caused by the diffraction loss and the quality factor caused by the coupled cavity wall loss, and a better parameter for describing the

stability can be defined as

$$S = \frac{1/Q_{\rm t} - 1/Q_{\rm c}}{1/Q_{\rm c}} = \frac{Q_{\rm c}}{Q_{\rm b}}, \tag{7}$$

where $1/Q_{\rm t} = 1/Q_0 + 1/Q_{\rm e} + 1/Q_{\rm b}$, with $Q_{\rm t}$ being the total quality factor for the beam–cavity system, $1/Q_{\rm c} = 1/Q_0 + 1/Q_{\rm e}$, and $Q_{\rm c}$ the non-beam-loaded quality factor of the coupled cavity chain.

It can be seen from formula (7) that if $S > 0$, then the beam absorbs the energy from the gap electric field, and the system will keep the stability no matter whether there is an external load for the system, if $-1 < S < 0$, i.e., if $Q_{\rm c} < |Q_{\rm b}|$, then the external load and the coupled cavity wall can fully absorb the energy released by the beam, and the system still keeps the stability; if $S < -1$, i.e., $Q_{\rm c} > |Q_{\rm b}|$, then the system is unstable.

3.2. Stability of the 2π mode operation

There are five modes in a three-gap coupled cavity chain (Fig. 1): the π mode, $\pi/2$ mode, 2π mode, $\pi/2$ slot mode, and π slot mode. As an application example, the calculations will be performed in the operating frequency range of the Ku band

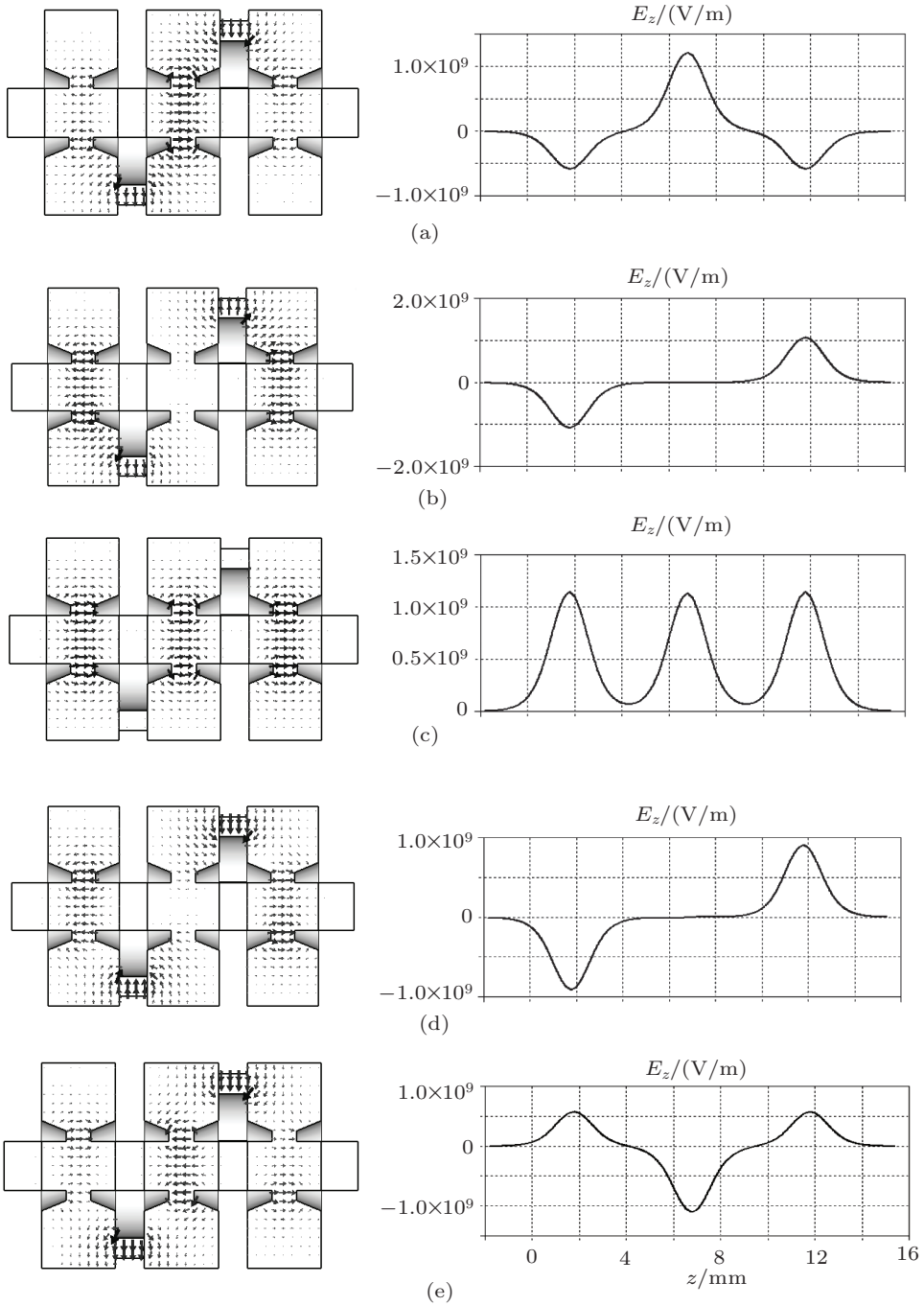


Fig. 2. Electric field distributions in a three-gap Hughes-type coupled cavity chain for different modes: (a) π mode, $f = 13.86$ GHz, (b) $\pi/2$ mode, $f = 15.62$ GHz, (c) 2π mode, $f = 16.56$ GHz, (d) $\pi/2$ slot mode, $f = 23.83$ GHz, (e) π slot mode, $f = 25.91$ GHz.

with the same distance between the adjacent gaps, l. The corresponding geometrical parameters are listed in Table 1. Table 2 gives the "cold" parameters of the five modes, calculated with the CST code for the three-gap coupled cavity chain, such as resonant frequencies, gap voltages, and characteristic impedance. Figure 2 shows the vector patterns of the electrical field in the coupled cavity chain and the curve of the electric field profile in the axial direction at the cylindrical center.

Table 1. The geometrical parameters of the three-gap cavity chain for the 2π mode operation.

r_a/mm	r_c/mm	r_d/mm	r_s/mm	r/mm	d/mm	d_s/mm	t/mm	l/mm	θ/(°)
1.2	2.2	1.7	3.4	4.9	1.2	2.4	1.4	5.0	130

Table 2. The "cold" parameters of the different modes for the 2π mode operation.

Mode name	f/GHz	Amplitude of the gap voltages			Characteristic impedance/Ω
		V_1	V_2	V_3	
π mode	13.86	–1.35	3.09	–1.35	192.48
$\pi/2$ mode	15.62	–2.76	0.00	2.76	155.23
2π mode	16.56	2.51	2.48	2.51	256.08
$\pi/2$ slot mode	23.83	–1.11	0.00	1.11	16.46
π slot mode	25.91	0.87	–1.62	0.87	34.67

It can be seen from Fig. 2 that the first and fifth modes are π mode, in which the electric field intensity on the middle gap is obviously stronger than that on the other gaps, the directions of the electric fields in the adjacent gaps are opposite, the amplitudes of the radial electric field on the two coupling slots are equal and their directions are the same, and the characteristic impedances of the modes are, respectively, 192.48 Ω and 34.76 Ω (as shown in Table 2). The first mode is called the π mode and the fifth mode is named the π slot mode. The electric field intensity of the π mode on the gap is higher than that of the π slot mode. The electric field on the middle gap is almost zero for the second and fourth modes, the amplitudes of the electric field on the first and third gaps are equal and their directions are opposite, there are strong electric fields on the two coupling slots and their directions are opposite, and the characteristic impedances of the modes are, respectively, 155.23 Ω and 16.46 Ω. The second mode is called the $\pi/2$ mode and the fourth mode is named the $\pi/2$ slot mode. The electric field intensity of the $\pi/2$ mode on the gap is higher than that of the $\pi/2$ slot mode. For the third mode, the electric fields on three gaps are almost equal and their directions are the same, there are almost no electric fields on the two coupling slots, and the characteristic impedance of the mode is 256.08 Ω. This is usually called the 2π mode, and has the largest characteristic impedance in the five modes.

Because the geometrical size of each gap remains the same and the shape of the longitudinal electric field near the gap varies very little (only the amplitude of the electric field varies), the coupling coefficients of the single gap for different cavity units can be considered to be identical, i.e., $M_{g,n} = M_g$. The M_N may be a complex number, and usually the square of its modulus $|M_N|^2$ is used to indicate the coupling intensity between the beam and the gap electric field. From Eq. (6), the $|M_3|^2$ for the three-gap coupled cavity chain can be written as

$$|M_3(\beta)|^2 = \left|M_g(\beta)\right|^2 |\Phi_3(\beta)|^2, \tag{8}$$

where

$$|\Phi_3(\beta)|^2 = \frac{V_1^2 + V_2^2 + V_3^2 + 2V_1V_2\cos(\beta l) + 2V_2V_3\cos(\beta l) + 2V_1V_3\cos(2\beta l)}{(|V_1| + |V_2| + |V_3|)^2}.$$

If the direction of the electric field on the first gap is considered as the positive direction, the $|\Phi_3(\beta)|^2$ of π mode and the π slot mode can be expressed as

$$|\Phi_3(\beta)|^2 = \frac{V_1^2 + V_2^2 + V_3^2 - 2|V_1||V_2|\cos(\beta l) - 2|V_2||V_3|\cos(\beta l) + 2|V_1||V_3|\cos(2\beta l)}{(|V_1| + |V_2| + |V_3|)^2}. \tag{9}$$

When $\beta l = (2m-1)\pi$, $|\Phi_3(\beta)|^2_{\max} = 1$, and $|M_3|^2 = \left|M_g\right|^2$, the $|\Phi_3(\beta)|^2$ of the $\pi/2$ mode and the $\pi/2$ slot mode can be expressed as

$$|\Phi_3(\beta)|^2 = \frac{V_1^2 + V_3^2 - 2|V_1||V_3|\cos(2\beta l)}{(|V_1| + |V_3|)2}. \tag{10}$$

When $\beta l = (2m-1)\pi/2$, $|\Phi_3(\beta)|^2_{\max} = 1$, and $|M_3|^2 = \left|M_g\right|^2$, the $|\Phi_3(\beta)|^2$ of the 2π mode can be expressed as

$$|\Phi_3(\beta)|^2 = \frac{V_1^2 + V_2^2 + V_3^2 + 2|V_1||V_2|\cos(\beta l) + 2|V_2||V_3|\cos(\beta l) + 2|V_1||V_3|\cos(2\beta l)}{(|V_1| + |V_2| + |V_3|)^2}. \tag{11}$$

When $\beta l = 2m\pi$, $|\Phi_3(\beta)|^2_{\max} = 1$, and $|M_3|^2 = |M_g|^2$, the reciprocal of the beam quality factor for the three-gap coupled cavity chain Q_b can be written as

$$1/Q_b = G_b(R/Q) = \frac{(R/Q)}{4Z_0}(|M_3(\beta_e - \beta_q)|^2 - |M_3(\beta_e + \beta_q)|^2). \quad (12)$$

Based on formulae (8)–(12) and all the parameters given in Tables 1 and 2, the $1/Q_b$ can be calculated for the three-gap coupled cavity chain with the electron beam of the radius $r_b = 0.8$ mm and $P_{er} = 1.0$ μP or 2.0 μP (1 P = 0.1 Pa·s). The calculation results are given in Table 3 and Fig. 3.

It can be seen from Table 3 that if the three-gap coupled cavity chain is used as the input cavity or bunching cavity, the values of $1/Q_b$ of all modes are positive when the beam voltage is selected as 20 kV, which means no self-excited oscillation may happen. Figure 3 shows plots of $1/Q_b$ versus beam voltage for $P_{er} = 1.0$ μP and $P_{er} = 2.0$ μP. If the three-gap coupled cavity chain is used as the output cavity, $1/Q_b$ of the operational mode (2π mode) must be negative, the values of $1/Q_b$ of the other modes must be positive and the amplitude of $1/Q_b$ for the operational mode should be as large as possible under the condition of the operational mode stabilization. When the beam voltage is selected to be 29 kV, $1/Q_b$ of the operational mode is negative and its amplitude reaches maximum. $1/Q_b$ of the π mode always remains positive and its amplitude is relatively large. This is the most stable mode. The resonant frequency of the $\pi/2$ mode is close to that of the 2π mode and its characteristic impedance is also relatively large, but its $1/Q_b$ always remains positive in a beam voltage range from 7.7 kV to 32.5 kV. Although the values of $1/Q_b$ of the π slot mode and the $\pi/2$ slot mode may be negative near 29 kV, their amplitudes are at least one order of magnitude less than that of the 2π mode, which means that their self-excited oscillation can easily be suppressed with distributed wall losses. The difference between the beam voltage for stable operation and that for the case of serving as an output cavity can be adjusted by using different cavity lengths for the input/bunching cavity and output cavity, which can achieve good beam–wave interactions in a stably operational state.

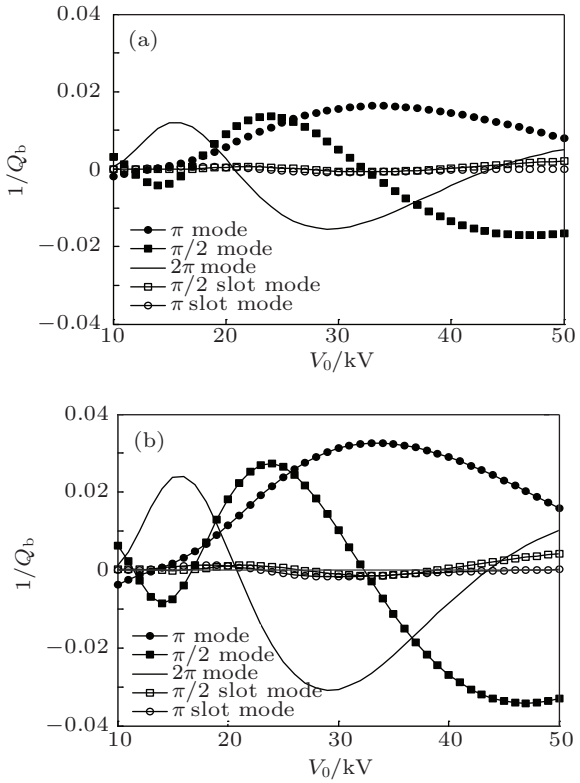


Fig. 3. Plots of $1/Q_b$ versus beam voltage for different values of perveance for the 2π mode operation with $r_b = 0.8$ mm: (a) $P_{er} = 1.0$ μP, (b) $P_{er} = 2.0$ μP.

Table 3. Values of $1/Q_b$ of five modes for the 2π mode operation.

V/kV	P_{er}/μP	π mode/10^{-3}	$\pi/2$ mode/10^{-3}	2π mode/10^{-3}	$\pi/2$ slot mode/10^{-3}	π slot mode/10^{-3}
20.00	1.00	5.45	9.98	3.32	0.615	0.694
29.00	1.00	0.156	8.30	–0.170	–0.546	–1.00
20.00	2.00	0.115	0.182	5.28	1.00	1.04
29.00	2.00	0.303	0.145	–0.309	–0.837	–1.67

Figure 4 shows the curves of $1/Q_b$ versus beam voltage with different beam radii for the 2π mode operation. It can be seen from Fig. 4 that the beam–wave coupling augments with the increase in the beam radius, the voltage range for keeping stable operation becomes slightly narrow, and the voltage as the output cavity for maximum $|1/Q_b|$ may be slightly low. The calculations show that there are also similar characteristics for the other four modes. This may be because the variation in r_b is more correlative to the beam wave coupling intensity and affects the beam–wave synchronization less.

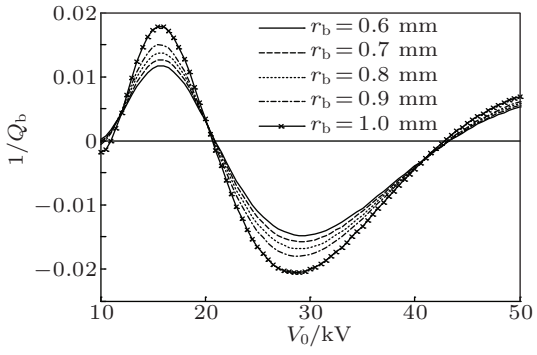


Fig. 4. Curves of $1/Q_b$ versus beam voltage with different beam radii for the 2π mode operation.

3.3. Stability of π mode operation

When the π mode at the first harmonic is selected as the operating mode, the difference in the phase of the electric field between the adjacent gaps is π. The transit-phase of the beam is decreased by half compared with that in the case of 2π mode operation, so the beam voltage needs to be increased or the periodicity length has to be cut down to keep the synchronization between the beam and the electric field. Table 4 gives the geometrical parameters of the three-gap coupled cavity chain for the π mode operation in the frequency range of the Ku band, and the "cold" parameters calculated with the CST code are shown in Table 5. Based on formulae (8)–(12) and all the parameters given in Tables 4 and 5, the calculation results of $1/Q_b$ are given in Table 6 and Fig. 5.

It can be seen from Table 6 that the values of $1/Q_b$ for all the modes are positive when the beam voltage is selected to be 34 kV, which means that no self-excited oscillation may happen. Figure 5 shows the curves of $1/Q_b$ versus beam voltage for $P_{er} = 1.0$ μP and $P_{er} = 2.0$ μP. If the three-gap coupled cavity chain is used as the output cavity, when the beam voltage is selected to be 81 kV, the value of $1/Q_b$ for the operational mode (π mode) is negative and its amplitude reaches a maximum, and the values of $1/Q_b$ for the other modes are all positive, and the system can remain stable. However, the beam voltage as the output cavity is twice as large as that for keeping stable operations of all the modes, which may make the size of the output cavity so small that it is difficult to realize. In addition, it should be noted that when the beam voltage 40.0 kV $< V_0 <$ 78.0 kV, then the values of $1/Q_b$ for the π mode, 2π mode, and $\pi/2$ slot mode are all negative, and beam–wave interactions can happen for the π mode and the 2π mode at the first harmonic at the same time. The effect of the $\pi/2$ slot mode can be suppressed by load loss, whose $1/Q_b$ is at least one order of magnitude less than those in the cases of the π mode and 2π mode operation.

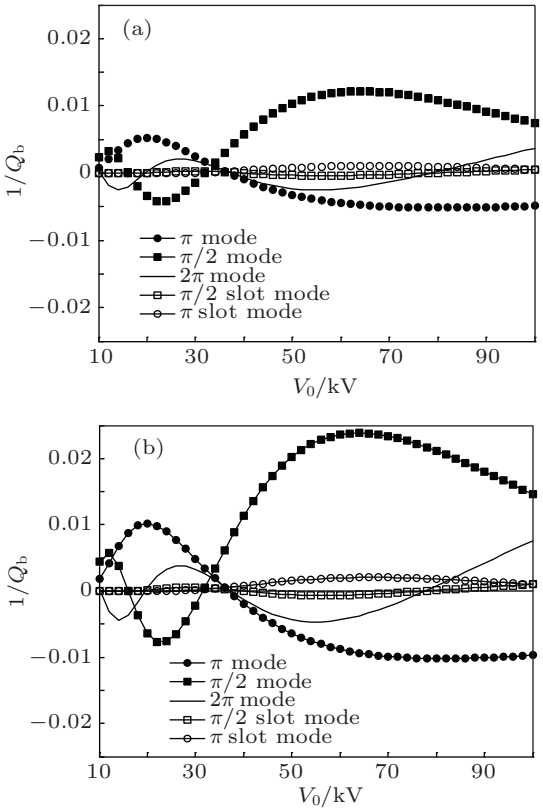


Fig. 5. Curves of $1/Q_b$ versus beam voltage for different values of perveance for π mode operation with $r_b = 0.8$ mm and $P_{er} = 1.0$ μP: (a) $P_{er} = 1.0$ μP and (b) $P_{er} = 2.0$ μP.

Table 4. The geometrical parameters of the three-gap cavity chain for the π mode operation.

r_a/mm	r_c/mm	r_d/mm	r_s/mm	r/mm	d/mm	d_s/mm	t/mm	l/mm	θ/(°)
1.2	2.2	1.7	3.95	5.2	1.2	1.5	0.4	3.0	85

Table 5. The "cold" parameters of the different modes for the π mode operation.

Mode name	f/GHz	Amplitude of the gap voltages			Characteristic impedance/Ω
		V_1	V_2	V_3	
π mode	16.52	–1.25	2.61	–1.25	125.78
$\pi/2$ mode	17.76	–2.62	0.00	2.62	123.03
2π mode	18.48	2.37	2.31	2.37	214.03
$\pi/2$ slot mode	27.83	–0.77	0.00	0.77	6.78
π slot mode	30.44	0.57	-1.12	0.57	13.35

Table 6. The $1/Q_b$ values of the five modes for the π mode operation.

V/kV	P_{er}/μP	π mode/10^{-3}	$\pi/2$ mode/10^{-3}	2π mode/10^{-4}	$\pi/2$ slot mode/10^{-4}	π slot mode/10^{-4}
34.00	1.00	1.01	1.51	9.32	2.07	1.49
81.00	1.00	–5.15	0.107	3.85	0.637	9.21
34.00	2.00	0.194	3.34	0.164	3.58	3.46
81.00	2.00	–0.102	0.209	0.109	1.61	0.178

3.4. Stability of $\pi/2$ mode operation

When the $\pi/2$ mode at the first harmonic is selected as the operating mode, $\beta l = \pi/2$, then the corresponding synchronization voltage is very high (or the periodicity length is too short), which may result in some technological problems. So we suppose that the $\pi/2$ mode operates at the second harmonic, i.e. $\beta l = 3\pi/2$. Table 7 gives the geometrical parameters of the three-gap coupled cavity chain for the $\pi/2$ mode operation in the frequency range of the Ku band, and the "cold" parameters calculated with the CST code are shown in Table 8. Based on formulae (8)–(12) and all the parameters given in Tables 7 and 8, the calculating results of $1/Q_b$ are given in Table 9 and Fig. 6.

Table 7. The geometrical parameters of the three-gap cavity chain for the $\pi/2$ mode operation.

r_a/mm	r_c/mm	r_d/mm	r_s/mm	r/mm	d/mm	d_s/mm	t /mm	l/mm	θ/(°)
1.2	2.2	1.7	3.1	3.3	1.2	0.4	0.2	3.2	192

Table 8. The "cold" parameters of different modes for the $\pi/2$ mode operation.

Mode name	f/GHz	Amplitude of the gap voltages			Characteristic impedance/Ω
		V_1	V_2	V_3	
π mode	13.91	–0.96	1.93	–0.96	84.80
$\pi/2$ mode	16.65	–1.42	0.00	1.42	38.55
2π mode	26.25	2.98	3.01	2.98	243.92
$\pi/2$ slot mode	28.30	–3.21	0.00	3.21	115.90
π slot mode	31.33	1.60	–3.12	1.60	101.45

Table 9. The $1/Q_b$ values of the five modes for the $\pi/2$ mode operation.

V/kV	P_{er}/μP	π mode/10^{-3}	$\pi/2$ mode/10^{-3}	2π mode/10^{-4}	$\pi/2$ slot mode/10^{-4}	π slot mode/10^{-4}
14.50	1.00	3.50	0.591	28.3	6.30	0.591
23.00	1.00	1.91	–1.64	1.81	2.66	–1.34
14.50	2.00	6.79	1.00	55.5	8.17	0.708
23.00	2.00	3.69	–2.99	0.298	0.141	–2.74

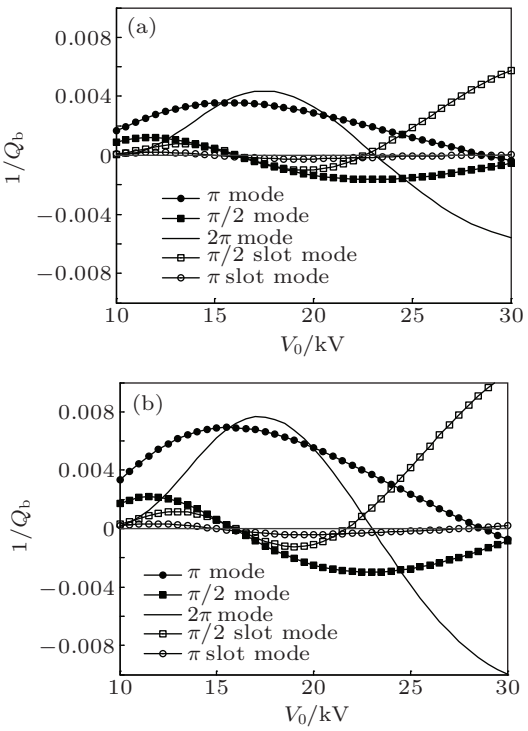


Fig. 6. Curves of $1/Q_b$ versus beam voltage for different values of perveance for $\pi/2$ mode operation with $r_b = 0.8$ mm and $P_{er} = 1.0$ μP: (a) $P_{er} = 1.0$ μP and (b) $P_{er} = 2.0$ μP.

It can be seen from Table 9 that the values of $1/Q_b$ for all modes are positive when the beam voltage is selected to be 14.50 kV, which means that no self-excited oscillation may happen. Figure 6 shows the curves of $1/Q_b$ versus beam voltage for $P_{er} = 1.0$ μP and $P_{er} = 2.0$ μP. If the three-gap coupled cavity chain is used as the output cavity, when the beam voltage is selected to be 23 kV, the value of $1/Q_b$ of the operational mode ($\pi/2$ mode) is negative and its amplitude reaches a maximum. Although the value of $1/Q_b$ for the π slot mode may be negative at 23 kV, its amplitude is one order of magnitude less than that in the case of $\pi/2$ mode operation, which means that their self-excited oscillations can easily be suppressed with distributed wall losses. However, the characteristic impedance of the $\pi/2$ mode is very small for this case. The calculations show that the characteristic impedance of the $\pi/2$ mode can be increased to larger than 100 Ω by adjusting the geometrical parameters of the coupled cavity chain, but the beam voltage for the stable operation will reduce and the beam voltage for the case serving as the output cavity will rise. In addition, it should be noted that when the beam voltage 16.0 kV $< V_0 <$ 22.0 kV, then the $1/Q_b$ values of the $\pi/2$ slot mode and π slot mode are all negative and the synchronizing voltage of the $\pi/2$ slot mode at the third harmonic is 14.93 kV. Beam–wave interaction may occur for the $\pi/2$ slot mode at the third harmonic as well as the π slot mode and the $\pi/2$ mode at the second harmonic at

same time, and the effect from the $\pi/2$ slot mode at the third harmonic may be more serious.

4. Conclusion

Starting from space-charge wave theory, the formulae of the beam–wave coupling coefficient $|M_N|^2$ and the beam-loaded conductance G_b are given for the beam–wave interaction in an N-gap Hughes-type coupled cavity chain with an electron beam. The ratio of the non-beam-loaded quality factor of the coupled cavity chain to the beam quality factor $S = Q_c/Q_b$ is used to determine its stability. The beam–wave interaction discussion for a three-gap Hughes-type coupled cavity chain with the formulae and CST code shows that the 2π mode, π mode, and $\pi/2$ mode may all operate stably in the EIK. No matter which mode is selected as the operating mode, the characteristic impedance of the 2π mode is always maximal in the three modes. For the 2π mode operation at the first harmonic, the difference between the beam voltage for stable operation and that for output cavity operation is the smallest, and the effects of the other modes on stability may easily be suppressed. Too large a difference between the beam voltage for the case serving as the output cavity and that for keeping stable operation may lead to some practical difficulties in realizing π mode stable operation. Although the beam voltage difference for the $\pi/2$ mode operation at the second harmonic can be reduced, its characteristic impedance will also fall obviously, and the possibility of parasitical mode oscillation increases.

References

[1] Wessel-Berg T 1957 *Microwave Laboratory, Stanford University, Technical Reports* p. 376

[2] Chodorow M and Wessel-Berg T 1961 *IRE Trans. Electron. Dev.* **8** 44

[3] Shin Y M and Park G S 2004 *J. Korean Phys. Soc.* **44** 1239

[4] Roitman A, Horoyski P, Berry D and Steer B 2006 *Proceeding of the Seventh IEEE International Vacuum Electronics Conference*, April 25–27, Monterey, California, USA, p. 191

[5] Roitman A, Berry D and Steer B 2005 *IEEE Trans. Electron. Dev.* **52** 895

[6] Chen L, Cheng F H, Wang J D, Yang C Y and Chu K R 2002 *Proceeding of the Third IEEE International Vacuum Electronics Conference*, April 23–25, Monterey, California, USA, p. 322

[7] Randall J P, Perring D and Nuth V R 1980 *Proceedings of the Conference on Vacuum Devices* **30** 455

[8] Nguyen K T, Pershing D E, Abe D K and Levush B 2006 *IEEE Trans. Plasma Sci.* **34** 576

[9] Preist D H and Leidigh W J 1963 *IEEE Trans. Electron. Dev.* **10** 201

[10] Lien E and Robinson D 1966 *Technical Report for United States Army Electronics Command*, No. ECOM-01362-F

[11] Quan Y, Ding Y G and Wang S Z 2009 *IEEE Trans. Plasma Sci.* **37** 30

[12] Pierce J R and Shepherd W G 1947 *J. Bell System Tech.* **26** 663

[13] Branch G M Jr 1961 *IRE Trans. Electron. Dev.* **8** 193

[14] Cui J, Luo J R, Zhu M and Guo W 2011 *Acta Phys. Sin.* **60** 051101 (in Chinese)

[15] Хайков А З 1974 *КЛИСТРОННЫЕУСИЛИТЕЛИ* (*Klystron Amplifiers*), Излательстыо Свяэь p. 93

[16] Kantrowitz F and Tammaru I 1988 *IEEE Trans. Electron. Dev.* **35** 2018

[17] Perring D, Philips G and Smith M J 1976 *Advisory Group for Aerospace Research and Development Conference Proceedings*, Hayes, England, May 1–8, p. 197